Ground Water Quality

Straining, Attachment, and Detachment of *Cryptosporidium* Oocysts in Saturated Porous Media

S. A. Bradford* and M. Bettahar

ABSTRACT

Accurate knowledge of the transport and deposition behavior for pathogenic *Cryptosporidium parvum* oocysts is needed to assess contamination and protect water resources. Experimental and modeling studies were undertaken to examine the roles of attachment, detachment, and straining on oocyst transport and retention. Saturated column studies were conducted using Ottawa aquifer sands (U.S. Silica, Ottawa, IL) with median grain sizes of 710, 360, and 150 μm. Decreasing the median sand size tended to produce lower effluent concentrations, greater oocyst retention in the sand near the column inlet, and breakthrough of oocysts at later times. Oocyst transport data also exhibited concentration tailing. Mathematical modeling of the oocyst transport data using fitted first-order attachment and detachment coefficients provided a satisfactory description of the observed effluent concentration curves, but a poor characterization of the oocyst spatial distribution. Modeling of these data using an irreversible straining term that is depth dependent provided a better description of the oocyst spatial distribution, but could not account for the observed effluent concentration tailing or late breakthrough times. A more physically realistic description of the data was obtained by modeling attachment, detachment, and straining. The percentage of total oocysts retained by straining was estimated from effluent mass balance considerations to be 68% for 710-μm sand, 79% for 360-μm sand, and 87% for 150-μm sand. Straining coefficients were then selected to achieve these percentages of total oocyst retention, and attachment and detachment coefficients were fitted to the effluent concentration curves. Dramatic differences in the predicted oocyst breakthrough curves were observed at greater transport distances for the various model formulations (inclusion or exclusion of straining). Justification for oocyst straining was provided by trends in the transport data, simulation results, pore size distribution information, and published literature.

Cryptosporidium parvum is a protozoan parasite that infects the intestines of a variety of wild and domesticated animals, as well as humans (Current, 1986). The infectious stage of this parasite is biologically dormant oocysts that are shed in high numbers within the feces of infected animals. *Cryptosporidium* oocysts are ubiquitous in surface water (Rose, 1988; Rose et al., 1991; LeChevallier et al., 1991; Hoogenboezem et al., 2001). Field surveys also indicate that low levels of oocyst contamination in ground water are rather frequent (Lisle and Rose, 1995; Hancock et al., 1997). Many outbreaks of cryptosporidiosis have been reported in industrialized countries (Craun, 1990; Craun et al., 1998). A single outbreak of cryptosporidiosis in 1993 caused illness in 370 000 individuals from Milwaukee, Wisconsin. Ingestion of contaminated water containing as few as 10 oocysts can lead to infection (Olson et al., 1999). Hence, contamination of drinking water by oocysts is a serious concern for public health.

Few commercial disinfectants are effective against oocysts in drinking water (Sobsey, 1989; Peeters et al., 1989), including chlorination at normal drinking water treatment levels. Riverbank filtration, infiltration basins and trenches, and sand filters are sometimes used to remove oocysts from surface water or effluent from sewage treatment. The efficacy of soil treatments depends on the retention and survival of oocysts in porous medium. Several published studies have examined transport and retention behavior of *Cryptosporidium* oocysts (Mawdsley et al., 1996a, 1996b; Brush et al., 1999; Harter et al., 2000; Logan et al., 2001). Mawdsley et al. (1996a, 1996b) found significant subsurface transport of oocysts in tilted soil boxes and undisturbed soil columns. These authors concluded that rapid flow of water through macropores largely bypasses the filtering and adsorptive effects of soil and increases the risk of oocyst transport to ground water. Brush et al. (1999) measured effluent concentration curves in several sands, and analyzed their data using an analytical solution to the transport equation that accounts for advection, dispersion, linear equilibrium sorption, and first-order decay. Harter et al. (2000) measured oocyst effluent concentration curves and spatial distributions in various sands at several transport velocities. The collected data were characterized using traditional clean-bed (first-order) attachment theory. Logan et al. (2001) also conducted oocyst transport experiments that examined the influence of water quality, sand size, and flow rate, and observed that the vast majority of oocyst retention occurred in the sand adjacent to the column inlet. Brush et al. (1999), Harter et al. (2000), and Logan et al. (2001) all observed trends of increasing oocyst retention with decreasing sand size.

The retention of colloids (such as oocysts) in porous media is typically ascribed to attachment (Ryan and Elimelech, 1996; Kretzschmar et al., 1999). Effluent concentration curves and spatial distributions of retained colloids in porous media, however, have not always been in agreement with colloid attachment theory (Camesano and Logan, 1998; Bolster et al., 1999; Redman et al., 2001; Bradford et al., 2002; Tufenkji et al., 2003). Some of these discrepancies have been attributed to soil surface roughness (Kretzschmar et al., 1997; Red-

S.A. Bradford, USDA-ARS, George E. Brown Jr. Salinity Laboratory, 450 W. Big Springs Road, Riverside, CA 92507-4617. M. Bettahar, Parsons, 100 West Walnut Street, Pasadena, CA 91124. Mention of trade names and company names in this manuscript does not imply any endorsement or preferential treatment by the USDA. Received 2 June 2004. *Corresponding author (sbradford@ussl.ars.usda.gov).

Published in J. Environ. Qual. 34:469–478 (2005).

677 S. Segoe Rd., Madison, WI 53711 USA

man et al., 2001) and charge variability (Johnson and Elimelech, 1995), heterogeneity in colloid characteristics (Bolster et al., 1999), colloid detachment (Tufenkji et al., 2003), time dependent attachment behavior (Johnson and Elimelech, 1995), and straining (Bradford et al., 2002, 2003).

Review of published oocyst transport studies (Mawdsley et al., 1996a, 1996b; Brush et al., 1999; Harter et al., 2000; Logan et al., 2001) indicates that straining was neglected or discounted as a mechanism for oocyst retention. Recently published colloid transport data (Bradford et al., 2002, 2003), however, indicate that straining may play a much more significant role in oocyst retention than was previously thought. Furthermore, little research attention has also been placed on oocyst detachment, although release of other colloids has frequently been reported (Meinders et al., 1995; Johnson et al., 2001). Knowledge of oocyst transport processes is further hampered by the experimental difficulties and costs associated with the tedious measurement of *Cryptosporidium* oocysts. For example, oocyst concentrations are typically determined by epifluorescent microscopic enumeration after staining with a fluorescent monoclonal antibody (Mawdsley et al., 1996a, 1996b; Brush et al., 1999; Harter et al., 2000; Logan et al., 2001). This staining and enumeration protocol can frequently take as much as one to two labor-intensive hours per sample. Accurate description and modeling of oocyst retention processes is therefore essential to predict transport behavior and vulnerability of water resources to oocyst contamination.

The primary objective of this research is to examine the roles of straining, attachment, and detachment in oocyst transport and deposition. The influence of sand grain size distribution characteristics on oocyst transport was also investigated. Transport and retention of oocysts in saturated column experiments were assessed by measuring temporal changes in effluent concentrations and by studying the final oocyst spatial distributions in the columns. The data were interpreted with the aid of numerical simulations of the experimental systems that included oocyst straining, attachment, and detachment. Additional simulations were conducted at larger spatial and temporal scales to further elucidate the implications of the various oocyst transport model formulations.

MATERIALS AND METHODS

Live *Cryptosporidium* oocysts, suspended in phosphate buffered saline solution, were obtained from Waterborne (New Orleans, LA). These oocysts were purified from manure of experimentally infected calves by sucrose and Percoll gradient centrifugation and water washes. The tracer solution in the transport experiments consisted of the oocyst suspension diluted in a solution of 0.001 *M* NaBr with its pH buffered to 6.73 using $NaHCO_3$ (5×10^{-5} *M*). The initial concentration (C_i) of oocysts in this solution was determined using the protocol described by Bradford and Schijven (2002). In brief, the oocysts were rinsed with a surfactant solution, concentrated by centrifugation, stained with an FITC monoclonal antibody, and enumerated using epifluorescent microscopy. Medema et al. (1998) reported that *Cryptosporidium parvum* oocysts ranged from 3.9 to 5.9 μm in diameter (mean value of 4.9 μm), and that their density was between 1.0 and 1.1 g cm^{-3} (geometric mean of 1.05 g cm^{-3}). Similarly, Waterborne reported that oocysts were approximately 3 to 5 μm in diameter. The oocyst electrophoretic mobility was measured to be -1.22 μm s^{-1} V^{-1} cm (corresponding to a zeta potential of -16.8 mV) in the 0.001 *M* NaBr solution using a ZetaPALs instrument (Brookhaven Instruments Corporation, Holtsville, NY).

The initial resident and eluant solutions in the transport experiments consisted of 0.001 *M* NaCl with its pH buffered to 6.98 using $NaHCO_3$ (5×10^{-5} *M*). The aqueous solvent for all experimental solutions was deionized water. The aqueous-phase chemistry (pH, ionic strength, and composition) of these solutions was chosen to create a mono-dispersed suspension with the oocysts.

Aquifer material used in the column experiments consisted of various sieve sizes of Ottawa (quartz) sand. The porous media were selected to encompass a range in grain sizes, and were designated by their median grain size (d_{50}) as 710, 360, and 150 μm. The uniformity index (d_{60}/d_{10}; here x% of the mass is finer than d_x) was 1.21 for the 710 μm sand, 1.88 for the 360 μm sand, and 2.25 for the 150 μm sand. Ottawa sands typically consist of 99.8% SiO_2 (quartz) and trace amounts of metal oxides, are spheroidal in shape, and have rough surfaces. The vast majority of the sands possess a net negative charge at a neutral pH.

Bradford and Abriola (2001) presented capillary pressure–saturation curves for the 710-, 360-, and 150-μm Ottawa sands. An estimate of the pore size distribution of drained pores can be obtained from capillary pressure–saturations curves using Laplace's equation of capillarity. Unfortunately, it is frequently difficult to characterize the small pores that may produce straining by this method because of the presence of residual water (due to discontinuity of the wetting films). Alternatively, Herzig et al. (1970) calculated the volume of spherical colloids that could be retained in pores based on geometric considerations. The percent volume retained by straining was calculated (assuming co-ordination number of 7, a porosity of 0.35, oocyst diameter of 5 μm, and grain diameter equal to d_{10}) to be 0.01% for the 710-μm sand, 0.09% for the 360-μm sand, and 1.00% for the 150-μm sand. Although these straining volumes are quite small, significant numbers of oocysts are required to fill these sites. For example, 2.8×10^{10} oocysts (5 μm) would be required to fill all the straining sites in uniform 150-μm sand packed in a column that is 10 cm long and has an inside diameter of 5 cm. This corresponds to complete retention of 5 μm oocyst in 10 600 L of suspension at a concentration of 2.6×10^6 oocysts L^{-1}.

The columns were 15-cm-long, 4.8-cm-i.d. Chromaflex chromatography columns (Kimble/Kontes, Vineland, NJ) made of borosilicate glass. The chromatography columns were equipped with a standard flangeless end fitting at the column bottom, and a flow adapter at the top. The flow adapter allowed the column bed length to be adjusted, thereby facilitating the tight sealing of the adapter at the sand surface. The manufacturer's bed support at the column inlet and outlet was replaced with a stainless steel wire screen (105-μm mesh spacing) to uniformly distribute water flow and oocysts at the sand surfaces. Tubing to and from the columns, fittings, column o-rings, and flow adapter were composed of chemically resistant materials such as Teflon, viton, stainless steel, and Kalrez.

The columns were wet-packed with the various porous media, with the water level always kept a few centimeters above the sand surface. Care was taken to ensure a uniform packing by completely mixing small quantities of the appropriate sieve size before addition to the columns. After each incremental addition of sand, the added sand was gently mixed with the lower surface layer of sand and then vibrated to minimize any

settling and layering, and to liberate any entrapped air. Table 1 provides porosity (ε) values for each experimental column. The porosity was determined according to the method of Danielson and Sutherland (1986) using the measured bulk density and assuming a specific solid density of 2.65 g cm^{-3}.

Before initiating a transport experiment the columns were flushed with several cycles of deionized water and 0.026 *M* NaCl to remove most of the natural colloids from the porous media. The columns were flushed as follows: initial resident solution was 0.026 *M* NaCl, 2 pore volume (PV) flush with deionized water, 2 PV flush with 0.026 *M* NaCl solution, 2 PV flush with deionized water, and finally a 4-PV flush with eluant solution. Here the 0.026 *M* NaCl solution promotes clay aggregation and the deionized water promotes clay mobilization (Bettahar et al., 1998). This treatment produced persistently low effluent concentrations of natural colloids in the column effluent.

Bradford et al. (2002) provides a schematic of an experimental setup that is similar in design to that used in the oocyst column studies. A Masterflex L/S drive pump (Barnant Company, Barrington, IL) was used to pump oocyst and bromide tracer or eluant solution upward through the vertically oriented columns at a steady rate. The average Darcy velocities (q) for the various column experiments are given in Table 1. The oocyst and bromide tracer solution was pumped through the columns for about 80 min (about 2 PV), after which a three-way valve was used to switch the pumped solution to the eluant for a total experimental time of 250 min (about 6.3 PV). Twenty-five effluent samples (10-min intervals) were collected from each column and analyzed for oocyst concentration using the previously discussed enumeration protocol. Bromide concentrations were determined on these same samples using an Orion 720a pH/ISE meter (Orion Research, Beverly, MA) until the bromide pulse was recovered.

Following completion of the transport experiments, the spatial distribution of oocysts in the column was determined. The end fitting was removed and the saturated porous medium was carefully excavated into 50-mL polypropylene vials. Approximately 10 vials were recovered from a column, with each vial containing about 40 g of sand (corresponding to a depth increment of about 1.2 cm). The remaining volume of the vials was filled with 0.001 *M* NaBr solution. The vials were shaken for 15 min using a Eberbach shaker (Eberbach Corporation, Ann Arbor, MI). The concentration of oocysts in the excess 0.001 *M* NaBr solution was then determined using the previously discussed oocyst enumeration protocol. Liquid- and sand-filled vials were placed in an oven (100°C) overnight to volatilize the remaining solution from the sand. The volume of solution and mass of sand in each vial was determined from mass balance by measuring the weight of the empty vials, liquid- and sand-filled vials, and sand-filled vials.

A batch experiment was conducted to determine the efficiency of oocyst release from the sand. A worst case retention scenario was considered by placing 15 g of the finest 150-μm sand and 10 mL of the initial oocyst suspension into a 20-mL glass scintillation vial. The suspension and sand were allowed to equilibrate for 4 h while being continuously mixed with an orbital shaker. The final concentration of the oocyst suspension was then measured using the outlined enumeration procedure. The initial and final oocyst concentrations were within the range of replicate initial oocyst concentrations, suggesting a high release efficiency for oocysts from the Ottawa sands.

An oocyst number balance was conducted at the end of each column experiment using the effluent concentration data and the final spatial distribution of retained oocysts in the sands. The calculated number of effluent and sand retained oocysts was normalized by the total number of injected oocysts into a column. Table 1 presents the calculated effluent (F_e), sand (F_s), and the total ($F_t = F_e + F_s$) number fractions recovered for the experimental systems.

Table 1. Column properties (Darcy velocity, q; porosity, ε; and column length, L_c) and the recovered effluent (F_e), sand (F_s), and the total (F_t) oocyst number fractions.

Soil size	ε	q	L_c	F_e	F_s	F_t
μm		cm min^{-1}	cm			
710	0.36	0.11	13.0	0.43	0.59	1.02
360	0.34	0.10	12.6	0.21	0.63	0.84
150	0.35	0.13	12.7	0.14	1.16	1.30

THEORY

The aqueous-phase oocyst mass balance equation is written herein as:

$$\frac{\partial(\theta_w C)}{\partial t} = -\nabla \cdot J_T - E_{sw}^{att} - E_{sw}^{str} \quad [1]$$

where C (N L_e^{-3}; N denotes number and L_e length) is the oocyst concentration in the aqueous phase, t (T) is time, θ_w (dimensionless) is the volumetric water content, J_T (N L_e^{-2} T^{-1}) is the total oocyst flux (sum of the advective, dispersive, and diffusive fluxes), E_{sw}^{att} (N L_e^{-3} T^{-1}) is the oocyst mass transfer terms between the aqueous and solid phases due to attachment, and E_{sw}^{str} (N L_e^{-3} T^{-1}) is the oocyst mass transfer terms between the aqueous and solid phases due to straining.

Clean-bed attachment–detachment theory has frequently been used to describe colloid interactions with porous media as (Bolster et al., 1999; Tufenkji et al., 2003):

$$E_{sw}^{att} = \frac{\partial(\rho_b S_{att})}{\partial t} = \theta_w k_{att} C - \rho_b k_{det} S_{att} \quad [2]$$

where S_{att} (N M^{-1}, M denotes mass) is the solid-phase concentration of attached oocysts, k_{att} (T^{-1}) is the first-order oocyst attachment coefficient, k_{det} (T^{-1}) is the first-order oocyst detachment coefficient, and ρ_b (M L_e^{-3}) is the sand bulk density.

Straining is modeled according to the approach described in Bradford et al. (2003). The mass balance equation for strained oocysts is given as:

$$E_{sw}^{str} = \frac{\partial(\rho_b S_{str})}{\partial t} = \theta_w k_{str} \psi_{str} C \quad [3]$$

where k_{str} (T^{-1}) is the straining coefficient, ψ_{str} (dimensionless) is a dimensionless oocyst straining function, and S_{str} (N m^{-1}) is the solid-phase concentration of strained oocysts. The value of ψ_{str} is a function of distance and is described as:

$$\psi_{str} = \left(\frac{d_{50} + z}{d_{50}}\right)^{-\beta} \quad [4]$$

where β (dimensionless) is a parameter that controls the shape of the oocyst spatial distribution, and z (L_e) is the distance from the column inlet. Equation [4] assumes that oocyst retention by straining occurs primarily at the column inlet because oocysts are retained in dead-end pores that are smaller than some critical size. The number of dead-end pores is hypothesized to decrease with increasing distance because size exclusion and/or limited advection and transverse dispersivity tend to keep mobile oocysts within the larger networks, thus bypassing smaller pores. Bradford et al. (2003) found that the value of $\beta = 0.432$ in Eq. [4] gave a good description of the spatial distribution of retained carboxyl latex colloids ($d_c/d_{50} < 0.02$; where d_c is the colloid diameter) when significant straining occurred. The value of β was therefore set equal to 0.432 for

all straining simulations because of the similar experimental conditions (aqueous chemistry and Ottawa sands) and range in d_c/d_{50} (<0.03) values, and so that the comparison between the various oocyst transport models will be based on the same data (effluent curves).

The HYDRUS-1D computer code (Simunek et al., 1998; Bradford et al., 2003) that accounts for both oocyst attachment, detachment, and straining (Eq. [1]–[4]) was used to analyze oocyst transport data. HYDRUS-1D simulates water, heat, and multiple solute movement in one-dimensional variably saturated porous media. The code is coupled to a nonlinear least squares optimization routine based on the Marquardt–Levenberg algorithm (Marquardt, 1963) to facilitate the estimation of transport parameters from experimental data. To test the ability of the models to predict oocyst spatial distributions, only effluent data were considered during parameter fitting. Values for the hydrodynamic dispersivity that were used in the simulations were taken from homogeneous column studies that used the same Ottawa sands, 3.2-μm carboxyl latex colloids, and a similar transport velocity (Bradford et al., 2002).

RESULTS AND DISCUSSION

Figure 1 presents plots of the *Cryptosporidium* oocyst effluent concentration curves in the indicated 710-μm (Fig. 1a), 360-μm (Fig. 1b), and 150-μm (Fig. 1c) sands. Here the relative effluent concentrations ($C\ C_i^{-1}$) are plotted as a function of pore volumes. The value of C_i was measured to be 2607 oocysts mL^{-1}. Figure 2 presents the corresponding spatial distributions of retained oocysts for the various sands (Fig. 2a for 710-μm sand, Fig. 2b for 360-μm sand, and Fig. 2c for 150-μm sand). The normalized concentration (number of oocysts, N_o, divided by the total number added to the column, N_{to}) per gram of dry sand is plotted as a function of dimensionless depth (distance from column inlet divided by the column length) in this figure. The recovered effluent, sand, and total oocyst number fractions shown in Table 1 indicate high oocysts recovery rates using the outlined experimental materials and protocols.

Figure 1 demonstrates that low effluent concentrations of oocysts (<32% of C_i) occurred for all of the sands. Decreasing the median sand size tended to produce lower effluent concentrations, greater oocyst retention (Table 1), and breakthrough of oocysts at later times. Oocyst transport data also exhibited concentration tailing. The spatial distribution of oocysts shown in Fig. 2 is highly dependent on the sand grain size. Increasing oocyst retention in the sand near the column inlet occurred with decreasing sand grain size. The coarser textured sands had slightly greater oocyst retention at a dimensionless depth of between 0.2 to 0.4 than the finer sands, but oocyst retention approached similar levels with increasing distance. The shape of the oocyst spatial distributions is generally consistent with that observed by Harter et al. (2000) and Logan et al. (2001).

Bradford et al. (2002) measured the transport behavior of 3.2-μm carboxyl latex microspheres using the same sands, eluant, and other column protocols used in this oocyst study. The peak breakthrough concentrations for the microspheres and oocysts were of a similar magnitude for a given sand (peak $C\ C_i^{-1}$ values for 3.2-μm microspheres were 0.43 in the 710-μm sand, 0.35 in the 360-μm sand, and 0.04 in the 150-μm sand). The shape of the oocyst and microsphere spatial distributions in a given sand was also alike. In contrast to oocyst transport, however, the microsphere breakthrough occurred at the same time as bromide and little detachment was observed. Differences in oocyst and microsphere breakthrough and concentration tailing are hypothesized to occur as a result of significant differences in the surface charge (−16.8 mV for oocysts and −57.25 mV for microspheres), concentration (2.7×10^3 oocyst mL^{-1} and 1.2×10^6 microspheres mL^{-1}), and size (3- to 6-μm oocyst and 3.2-μm microspheres).

The significant concentration tailing and late breakthrough time shown in Fig. 1 has not been reported in other published oocyst transport studies (Brush et al., 1999; Harter et al., 2000; Logan et al., 2001). Attachment and detachment of oocysts onto sand surfaces or onto previously retained oocysts (sand surfaces or in pores) are believed to control this tailing and late breakthrough behavior. A variety of chemical (electrostatic, London–van der Waals, hydration, hydrophobic, and steric forces), physical (hydrodynamics, sedimentation, and interception), and biological factors can play a role in oocyst–sand and oocyst–oocyst interactions (Ryan and Elimelech, 1996; Walker and Montemagno, 1999; Dai and Boll, 2003). These factors are typically lumped into attachment and detachment terms because it is difficult to separate the influence of the various processes. The column experiments were specifically designed to minimize chemical (simple aqueous and solid surface chemistries with repulsive electrostatic interactions between oocysts and quartz sands) and biological (clean sands and pure suspensions) factors on oocyst transport. To better characterize the relative importance of attachment, detachment, as well as straining in the transport experiments, data were simulated using various conceptual models.

Figures 1 and 2 also present plots of simulated effluent concentration curves (Fig. 1) and spatial distributions of retained oocysts (Fig. 2) in the various Ottawa sands. The simulation labeled Model-Att considered oocyst attachment as described in Eq. [1] and [2], with detachment and straining parameters set equal to zero. Table 2 shows fitted attachment parameter values, and statistical parameters (coefficient of linear regression and standard error) for the goodness of parameter fit to both effluent and spatial distribution data. The statistical parameters in Table 2 were used to assess the ability of the attachment model to describe the oocyst transport data. The effluent curve for the 710-μm sand was reasonably well described by the attachment model (Fig. 1a), although the concentration tailing is not accounted for in this model. The attachment model characterized the effluent concentration curves for the 360-μm (Fig. 1b) and 150-μm (Fig. 1c) sand systems poorly because it does not account for the late oocyst breakthrough. The attachment model also did a poor job of describing the spatial distribution of retained oocysts (Fig. 2), underestimating oocyst retention in the sand at the column inlet and overestimating oocyst retention at greater depths.

Attachment and detachment were considered in the model (Eq. [1] and [2], straining parameters were set

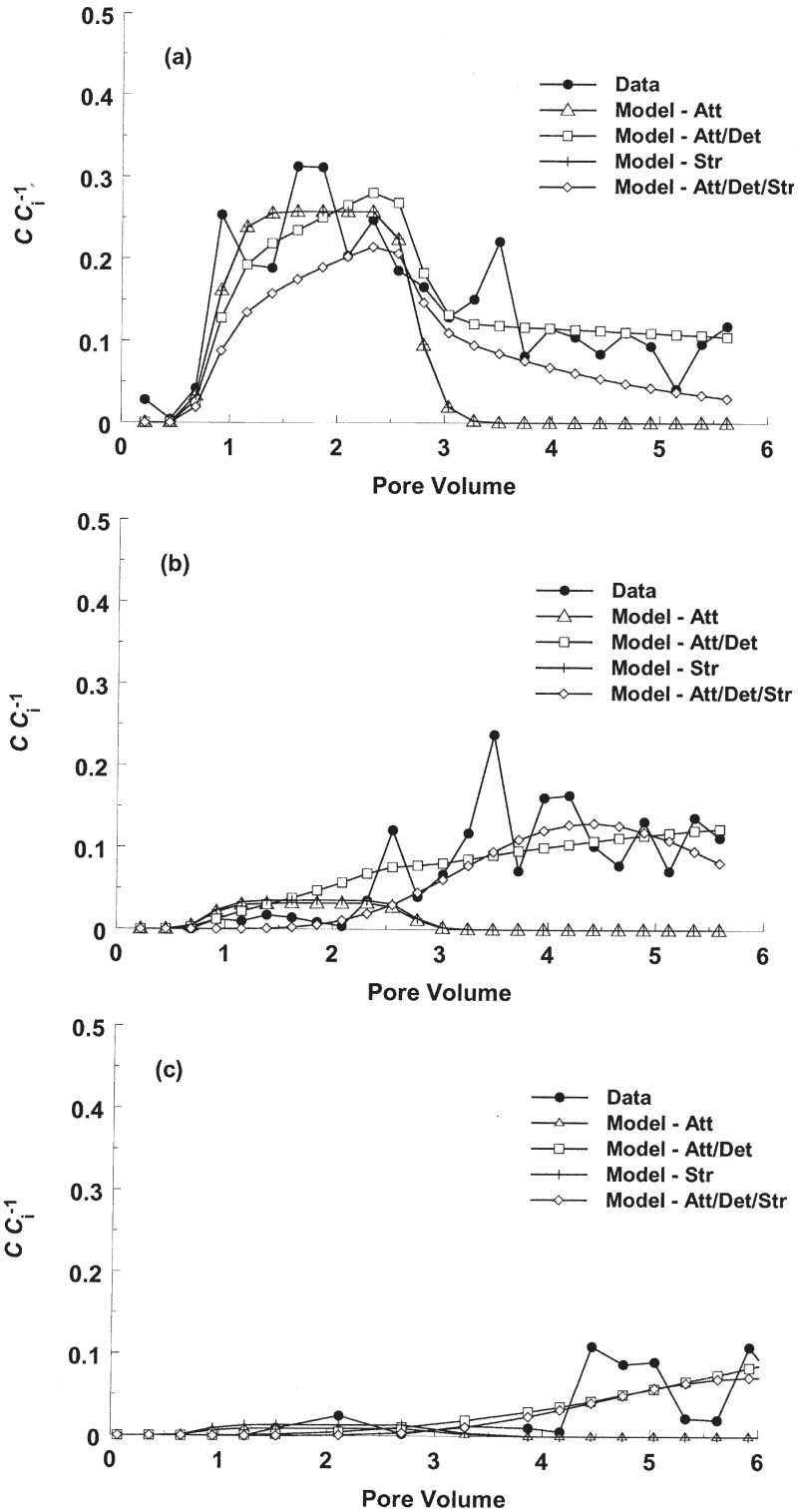

Fig. 1. Plots of observed and simulated *Cryptosporidium* oocyst effluent concentration curves in the (a) 710-μm, (b) 360-μm, and (c) 150-μm sands. Here relative effluent concentrations ($C\ C_i^{-1}$) are plotted as a function of pore volumes. Simulations considered attachment (Model-Att), attachment and detachment (Model-Att/Det), straining (Model-Str), and attachment, detachment, and straining (Model-Att/Det/Str). Corresponding spatial distributions of the retained oocysts in these sands are shown in Fig. 2. Fitted model parameters are presented in Table 2.

equal to zero) in an attempt to improve the simulation description. Figures 1 and 2 present plots of simulated effluent concentration curves (Fig. 1) and the spatial distributions of oocysts (Fig. 2) in the various Ottawa sands when using the attachment and detachment model (Model-Att/Det). Table 2 shows fitted attachment and detachment parameter values. Figure 1 and statistical parameters in Table 2 indicate that the attachment and

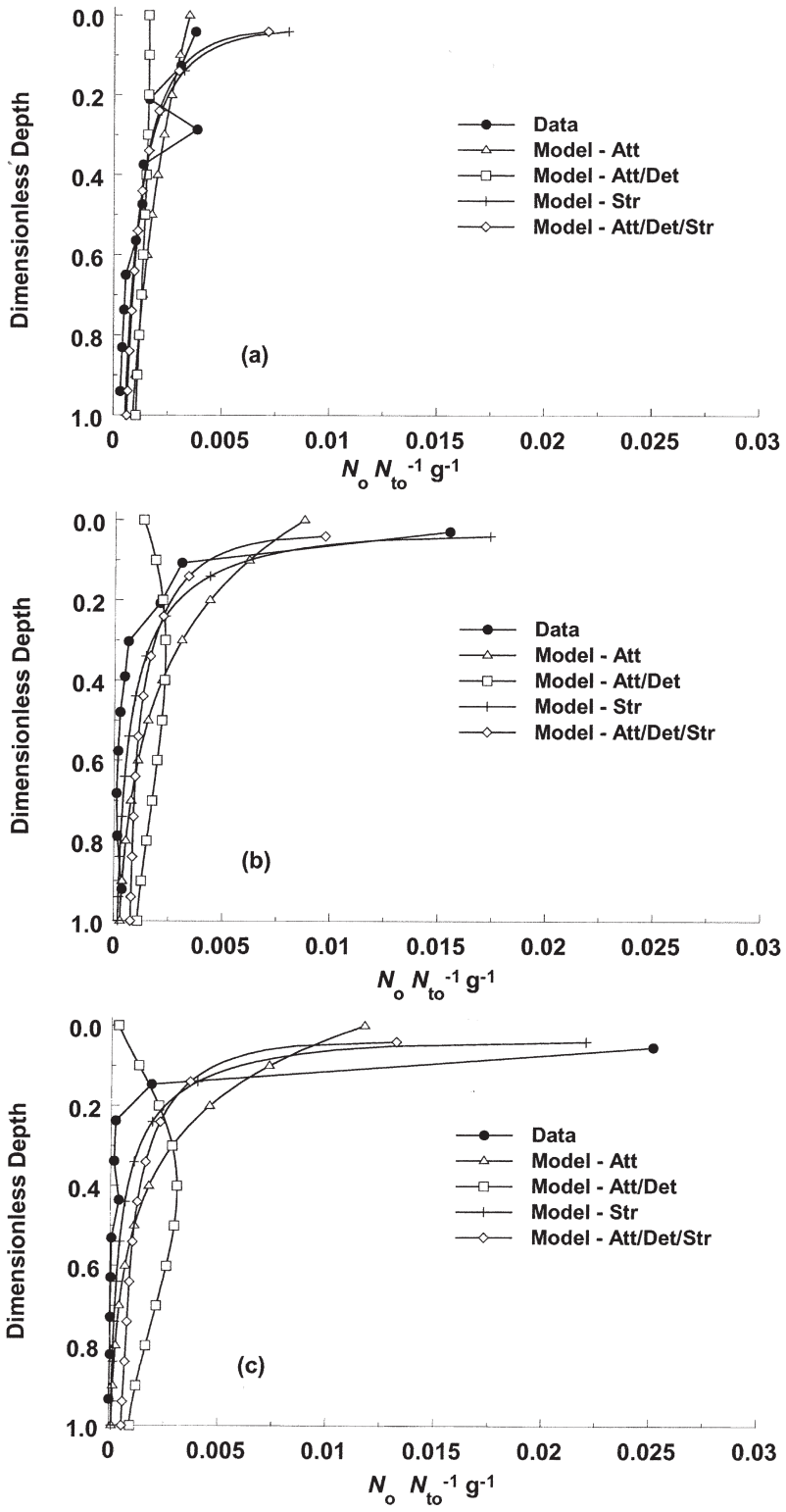

Fig. 2. Plots of observed and simulated spatial distributions of *Cryptosporidium* oocyst retained in the (a) 710-μm, (b) 360-μm, and (c) 150-μm sands. Here the normalized concentration ($N_o\ N_{to}^{-1}$) per gram of dry sand is plotted as a function of dimensionless depth (distance from column inlet divided by column length). Simulations considered attachment (Model-Att), attachment and detachment (Model-Att/Det), straining (Model-Str), and attachment, detachment, and straining (Model-Att/Det/Str). Corresponding oocyst effluent concentration curves are presented in Fig. 1. Fitted model parameters are presented in Table 2.

detachment model did a reasonable job at describing the effluent concentration curve, including concentration tailing. The descriptions of the oocyst spatial distributions were, however, more poorly characterized than the simulations that considered only attachment (Fig. 2 and Table 2). Inclusion of oocyst detachment produces

Table 2. Summary of the various fitted or estimated oocyst transport model parameters. Statistical parameters include the standard error (SE) and coefficient of linear regression for effluent (r_e^2) and spatial distribution (r_s^2) data (negative r^2 values were set equal to zero).

Model	Sand	Symbol	Value	SE	r_e^2	r_s^2
			—— min^{-1} ——			
Attachment (Att)	**710**	k_{att}	**0.035**	**15.22**	**0.529**	**0.000**
	360	k_{att}	**0.087**	**4.480**	**0.000**	**0.254**
	150	k_{att}	**0.150**	**0.678**	**0.000**	**0.422**
Att/detachment (Det)	**710**	k_{att}	**0.044**	**0.002**	**0.622**	**0.000**
		k_{det}	**0.005**	**0.001**		
	360	k_{att}	**0.110**	**0.017**	**0.218**	**0.000**
		k_{det}	**0.013**	**0.002**		
	150	k_{att}	**0.316**	**0.105**	**0.519**	**0.000**
		k_{det}	**0.029**	**0.012**		
Straining (Str)	**710**	k_{str}	**0.199**	**3.75**	**0.529**	**0.560**
	360	k_{str}	**0.625**	**7.68**	**0.000**	**0.988**
	150	k_{str}	**1.451**	**8.54**	**0.000**	**0.970**
Att/Det/Str	**710**	k_{att}	**0.027**	**0.009**	**0.678**	**0.561**
		k_{det}	**0.019**	**0.010**		
		k_{str}	**0.170**			
	360	k_{att}	**0.588**	**0.361**	**0.592**	**0.865**
		k_{det}	**0.200**	**0.128**		
		k_{str}	**0.280**			
	150	k_{att}	**1.638**	**0.802**	**0.410**	**0.824**
		k_{det}	**0.349**	**0.159**		
		k_{str}	**0.660**			

lower concentrations of oocysts in the sands near the column inlet and, hence, greater deviation from the experimental spatial distributions. Other researchers have observed deviations between attachment and detachment model predictions and experimental colloid transport data (Camesano and Logan, 1998; Bolster et al., 1999; Redman et al., 2001; Bradford et al., 2002; Tufenkji et al., 2003). It should be noted that Fig. 1 and 2 represent a best-case scenario for attachment–detachment (filtration) theory. Predicted oocyst transport behavior using published collector and sticking efficiencies would provide an even poorer description of these data.

Additional simulations were performed to explore the potential role of straining in oocyst retention. Initial simulations considered only straining (Eq. [1], [3], and [4]), with attachment and detachment parameters set equal to zero. Figures 1 and 2 present plots of simulated effluent concentration curves and the spatial distributions of oocysts in the various Ottawa sands when using the straining model (Model-Str). Table 2 shows fitted straining model parameter values. The straining model characterized the effluent concentration curves as well as the attachment model (Fig. 1 and Table 2), but did a much better job in characterizing the oocyst spatial distributions (Fig. 2 and Table 2). Concentration tailing and late breakthrough behavior were, however, not captured by the straining model.

The oocyst concentration tailing and late breakthrough behavior are consistent with an attachment–detachment retention mechanism (Fig. 1), whereas the oocyst spatial distributions suggest that straining is also occurring (Fig. 2). Analysis of published colloid transport data (Bradford et al., 2002, 2003) further supports the hypothesis that oocyst transport is influenced by attachment, detachment, and straining. Indeed, attachment of oocysts in small pores could induce straining. Simulations were therefore conducted that included these processes according to Eq. [1]–[4]. To avoid nonuniqueness problems in the parameter fits, the amounts of straining and attachment were estimated from the oocyst effluent concentration curves. Straining was modeled as an irreversible process in Eq. [3] and [4], and therefore cannot account for the observed concentration tailing and late oocyst breakthrough behavior. Mass balance determinations on the effluent concentration data in the tailing or late breakthrough regions were used to estimate the contribution of reversible attachment and irreversible straining. The percentage of total oocysts retained by straining was estimated to be 68% in the 710-μm sand, 79% in the 360-μm sand, and 87% in the 150-μm sand. Straining coefficients were selected to achieve these percentages of total oocyst retention. With the straining coefficients fixed to these values, the attachment and detachment coefficients were then fitted to the effluent concentration curves.

Figures 1 and 2 present plots of simulated effluent concentration curves (Fig. 1) and the spatial distributions of oocysts (Fig. 2) in the various Ottawa sands when using the attachment, detachment, and straining model (Model-Att/Det/Str). Table 2 shows fitted attachment and detachment model parameter values, as well as estimated straining parameters. The attachment, detachment, and straining model describes the effluent concentration curves and oocyst spatial distributions reasonably well. The percentage of total oocyst retention in the sand adjacent to the column inlet and outlet was calculated from the model output. Straining was observed to account for the vast majority of retention at the column inlet, whereas the importance of attachment on oocyst retention increased with increasing depth.

In summary, the trend of increasing oocyst retention in the sand near the column inlet with decreasing sand size (Fig. 2), the high oocyst recoveries in the sand (Table 1), and the simulation results (Fig. 1 and 2) all support the hypothesis that straining of oocysts occurred in the transport experiments. These observations are consistent with the reported finding that straining occurs for ratios of the colloid to median grain size greater than around 0.5% (Bradford et al., 2003). In this work the ratio of oocyst to median grain size is 0.7% for the 710-μm sand, 1.4% for the 360-μm sand, and 3.3% for the 150-μm sand.

Figures 1 and 2 indicate that the conceptual model used to describe oocyst transport and fate can significantly influence the predicted oocyst behavior at the column scale. At larger spatial and temporal scales the conceptual model for oocyst transport becomes even more important. To illustrate this point, Fig. 3 presents predicted effluent concentration curves (semi-log plot of relative effluent concentrations as a function of time) for oocysts in 710-μm sand at distances of 25, 50, and 100 cm from the inlet. Predictions were for the attachment–detachment (Eq. [1] and [2], with straining parameters set equal to zero) and the attachment–detachment–straining (Eq. [1]–[4]) conceptual models. In both cases, model parameters were determined by fitting (Table 2) to the experimental column data. Huge differences in the predicted breakthrough behavior occurred between

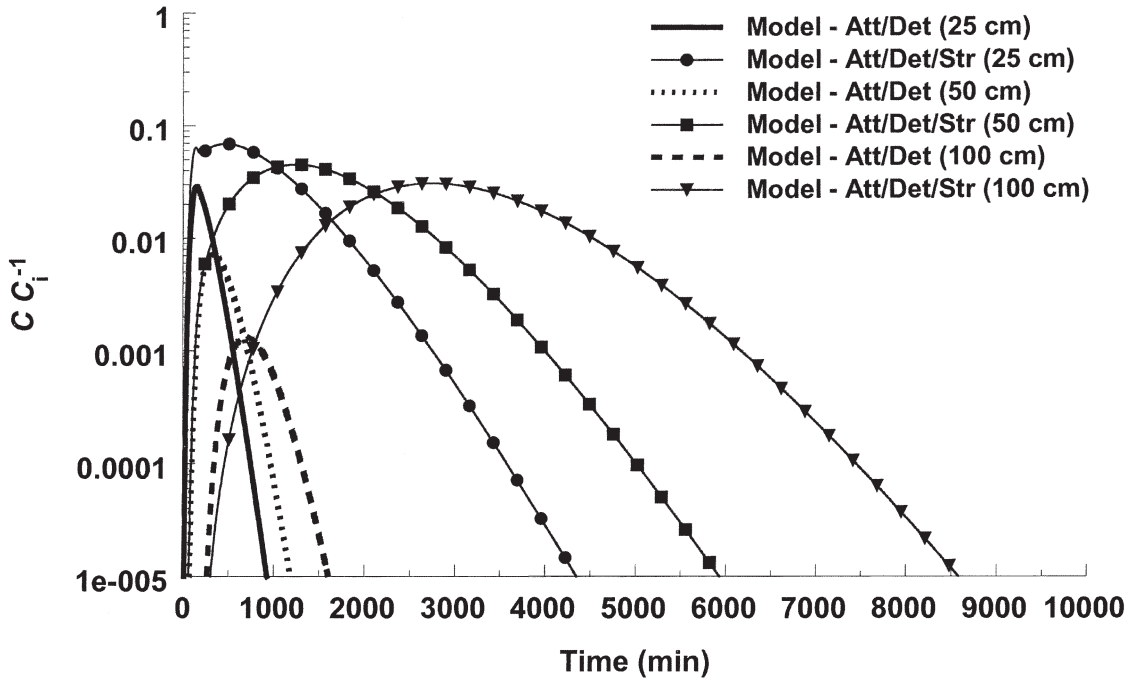

Fig. 3. Predicted effluent concentrations curves (semi-log plot of relative effluent concentrations as a function of time) for oocysts in 710-μm sand at distances of 25, 50, and 100 cm from the inlet. Predictions were obtained using the attachment–detachment (Model-Att/Det) and the attachment–detachment–straining (Model-Att/Det/Str) conceptual models. Model parameters were determined by fitting (Table 2) to the experimental soil column data.

the two conceptual models, especially with increasing distance. For example, at a distance of 100 cm the predicted relative concentrations for the attachment–detachment–straining model were more than an order of magnitude higher and breakthrough occurred more than five times longer than the attachment–detachment model. Recall that straining played an even more significant role in oocyst retention in the 360- and 150-μm sands compared with the 710-μm sand. Hence, differences in the conceptual model predictions were even greater for these finer sands. These longer-term simulations have important implications for other colloids that exhibit decreasing rates of colloid retention with increasing transport distance; such behavior has been observed in field and/or column studies using viruses (Pieper et al., 1997; Schijven et al., 1999; Redman et al., 2001), bacteria (Albinger et al., 1994; Martin et al., 1996; Baygents et al., 1998; Camesano and Logan, 1998; Simoni et al., 1998; Bolster et al., 1999), and latex microspheres (Bradford et al., 2002, 2004).

Straining has significant implications for oocyst transport in field soils. To further illustrate this point, consider the following example. Assume that the critical straining pore diameter for oocysts is 6 μm. This pore diameter can be related to a critical straining capillary pressure according to Laplace's equation of capillarity of about 490 cm of water pressure. The percentage of the pore space smaller than this critical straining pore diameter can then be calculated from measured capillary pressure curves and residual saturations using a capillary pressure–saturation curves model. Table 3 presents average parameter values for the capillary pressure–saturation model of van Genuchten (1980) for 12 major soil textural groups according to Carsel and Parrish (1988), as well as the calculated percentage of the pore space smaller than a critical straining pore diameter of 6 μm. Note that 10.5 to 91.8% of the pore space is calculated to have pores smaller than 6 μm in diameter for these soils.

CONCLUSIONS

Accurate knowledge of the processes that control *Cryptosporidium* oocysts transport and fate in saturated aquifer materials is needed to assess the vulnerability of water resources to contamination. Unfortunately, only a few studies have appeared in the literature on the transport and fate of oocysts, in part due to the costs and experimental difficulties associated with the tedious measurement of oocyst concentrations. Several column experiments were conducted to better elucidate the influence of attachment, detachment, and straining on oocyst migration. Previous oocyst transport studies have neglected or discounted straining as a mechanism of oocyst retention. Little research attention has also been given to oocyst detachment.

Decreasing the median sand size tended to produce lower effluent concentrations, greater oocyst retention in the sand near the column inlet, and breakthrough of oocysts at later times. Oocyst transport data also exhibited concentration tailing. Previous oocyst transport studies have not reported late breakthrough behavior and significant concentration tailing. Attachment and detachment of oocysts onto sand surfaces or onto previously retained oocysts (sand surfaces or in pores) provide one plausible explanation for this behavior.

Table 3. Average parameter values (residual water saturation, S_{rw}; reciprocal of the air entry pressure, α; empirical pore size distribution parameter, n; $m = 1 - 1/n$) for the capillary pressure–saturation model of van Genuchten (1980) for 12 major soil textural groups according to Carsel and Parrish (1988), as well as the calculated percentage of the pore space smaller than the critical straining pore diameter of 6 μm (PS_{str}).

Soil texture	S_{rw}	α	n	m	PS_{str}
		cm^{-1}			%
Sand	0.10	0.15	2.68	0.63	10.5
Loamy sand	0.14	0.12	2.28	0.56	14.4
Sandy loam	0.16	0.08	1.89	0.47	19.3
Loam	0.18	0.04	1.56	0.36	34.5
Silt	0.07	0.02	1.37	0.27	50.0
Silt loam	0.15	0.02	1.41	0.29	47.9
Sandy clay loam	0.26	0.06	1.48	0.32	40.4
Clay loam	0.23	0.02	1.31	0.24	61.2
Silty clay loam	0.21	0.01	1.23	0.19	74.4
Sandy clay	0.26	0.03	1.23	0.19	66.7
Silty clay	0.19	0.01	1.09	0.08	91.8
Clay	0.18	0.01	1.09	0.08	89.3

Mathematical modeling of the oocyst transport data using fitted attachment–detachment coefficients provided a satisfactory description of the effluent concentration curves, but a poor characterization of the oocyst spatial distribution. A more physically realistic description of the data was obtained by modeling attachment, detachment, and straining. Straining coefficients were calculated from effluent mass balance considerations, and attachment and detachment coefficients were fitted to the effluent concentration curves. According to this approach, irreversible straining accounted for 68% of the total oocysts in the 710-μm sand, 79% in the 360-μm sand, and 87% in the 150-μm sand. Dramatic differences in the predicted oocyst breakthrough curves were observed at greater transport distances for the various model formulations (inclusion or exclusion of straining). This suggests that characterization of oocyst retention mechanisms and associated conceptual models becomes more important with increasing transport distance.

Straining of oocysts occurs primarily at the sand surface and at textural interfaces when water flows from a coarser to a finer porous medium. Unsaturated water flow may also promote straining, when water is restricted to small pores as a result of capillary forces. Conversely, attachment is expected to play a significant role in oocyst retention in geochemically heterogeneous porous media and with increasing distance from the sand surface or textural interface. Additional research is justified to deduce the roles of various physical, chemical, and biological factors that are likely to influence attachment and straining behavior.

ACKNOWLEDGMENTS

This research was supported by the 206 Manure and Byproduct Utilization Project of the USDA-ARS.

REFERENCES

Albinger, O., B.K. Biesemeyer, R.G. Arnold, and B.E. Logan. 1994. Effect of bacterial heterogeneity on adhesion to uniform collectors by monoclonal populations. FEMS Microbiol. Lett. 124:321–326.

Baygents, J.C., J.R. Glynn, O. Albinger, B.K. Biesemeyer, K.L. Ogden, and R.G. Arnold. 1998. Variation of surface charge density in monoclonal bacterial populations: Implications for transport through porous media. Environ. Sci. Technol. 32:1596–1603.

Bettahar, M., O. Razakarisoa, F. van Dorpe, and M. Baviere. 1998. Influence of a surfactant decontamination technique on the hydraulic conductivity of a controlled aquifer polluted by diesel oil. Rev. Sci. Eau 11:85–100.

Bolster, C.H., A.L. Mills, G.M. Hornberger, and J.S. Herman. 1999. Spatial distribution of bacteria experiments in intact cores. Water Resour. Res. 35:1797–1807.

Bradford, S.A., and L.M. Abriola. 2001. Dissolution of residual tetrachloroethylene in fractional wettability porous media: Incorporation of interfacial area estimates. Water Resour. Res. 37:1183–1195.

Bradford, S.A., M. Bettahar, J. Simunek, and M.Th. Van Genuchten. 2004. Straining and attachment of colloids in physically heterogeneous porous media. Vadose Zone J. 3:384–394.

Bradford, S.A., and J. Schijven. 2002. Release of *Cryptosporidium* and *Giardia* from dairy calf manure: Impact of solution salinity. Environ. Sci. Technol. 36:3916–3923.

Bradford, S.A., J. Simunek, M. Bettahar, M.Th. van Genuchten, and S.R. Yates. 2003. Modeling colloid attachment, straining, and exclusion in saturated porous media. Environ. Sci. Technol. 37:2242–2250.

Bradford, S.A., S.R. Yates, M. Bettahar, and J. Simunek. 2002. Physical factors affecting the transport and fate of colloids in saturated porous media. Water Resour. Res. 38:1327, doi:10.1029/2002WR001340.

Brush, C.F., W.C. Ghiorse, L.J. Anguish, J.-Y. Parlange, and H.G. Grimes. 1999. Transport of *Cryptosporidium parvum* oocysts through saturated columns. J. Environ. Qual. 28:809–815.

Camesano, T.A., and B.E. Logan. 1998. Influence of fluid velocity and cell concentration on the transport of motile and nonmotile bacteria in porous media. Environ. Sci. Technol. 32:1699–1709.

Carsel, R.F., and R.S. Parrish. 1988. Developing joint probability distributions of soil water retention characteristics. Water Resour. Res. 24:755–769.

Craun, G.F. 1990. Waterborne giardiasis. p. 267–293. *In* E.A. Meyer (ed.) Human parasitic diseases. Vol. 3. Elsevier Sci. Publ., Amsterdam, the Netherlands.

Craun, G.F., S.A. Hubbs, F. Frost, R.L. Calderon, and S.H. Via. 1998. Waterborne outbreaks of cryptosporidiosis. J. Am. Water Works Assoc. 90:81–91.

Current, W.L. 1986. *Cryptosporidium*: Its biology and potential for environmental transmission. Crit. Rev. Environ. Control 17:21–51.

Dai, X., and J. Boll. 2003. Evaluation of attachment of *Cryptosporidium parvum* and *Giardia lamblia* to soil particles. J. Environ. Qual. 32:296–304.

Danielson, R.E., and P.L. Sutherland. 1986. Porosity. p. 443–461. *In* A. Klute (ed.) Methods of soil analysis. Part 1. 2nd ed. Agron. Monogr. 9. ASA and SSSA, Madison, WI.

Hancock, C.M., J.B. Rose, and M. Callahan. 1997. The prevalence of Cryptosporidium and *Giardia* in U.S. groundwaters. p. 147–152. *In* Proc. of 1997 Int. Symp. on Waterborne Cryptosporidium, Newport Beach, CA. 2–5 Mar. 1997. Am. Water Works Assoc., Denver.

Harter, T., S. Wagner, and E.R. Atwill. 2000. Colloid transport and filtration of *Cryptosporidium parvum* in sandy soils and aquifer sediments. Environ. Sci. Technol. 34:62–70.

Herzig, J.P., D.M. Leclerc, and P. LeGoff. 1970. Flow of suspension through porous media: Application to deep filtration. Ind. Eng. Chem. 62:129–157.

Hoogenboezem, W., H.A.M. Ketelaars, G.J. Medema, G.B.J. Rijs, and J.F. Schijven. 2001. *Cryptosporidium* and *Giardia*: Occurrence in sewage, manure and surface water. RIWA/RIVM/RIZA, Bilthoven, the Netherlands.

Johnson, P.R., and M. Elimelech. 1995. Dynamics of colloid deposition in porous media: Blocking based on random sequential adsorption. Langmuir 11:801–812.

Johnson, W.P., P. Zhang, P.M. Gardner, M.E. Fuller, and M.F. DeFlaun. 2001. Monitoring the response of indigenous bacteria to the arrival of injected bacteria using ferrographic capture. Appl. Environ. Microbiol. 67:4908–4913.

Kretzschmar, R., K. Barmettler, D. Grolimund, Y.-D. Yan, M. Borkovec, and H. Sticher. 1997. Experimental determination of colloid deposition rates and collision efficiencies in natural porous media. Water Resour. Res. 33:1129–1137.

Kretzschmar, R., M. Borkovec, D. Grolimund, and M. Elimelech.

1999. Mobile subsurface colloids and their role in contaminant transport. Adv. Agron. 66:121–193.
LeChevallier, M.W., W.D. Norton, and R.G. Lee. 1991. Occurrence of *Giardia* and *Cryptosporidium* spp. in surface water supplies. Appl. Environ. Microbiol. 57:2617–2621.
Lisle, J.T., and J.B. Rose. 1995. *Cryptosporidium* contamination of water in the USA and UK: A mini-review. J. Water SRT Aqua 44(3):103–117.
Logan, A.J., T.K. Stevik, R.L. Siegrist, and R.M. Ronn. 2001. Transport and fate of *Cryptosporidium parvum* oocysts in intermittent sand filters. Water Res. 35(18):4359–4369.
Marquardt, D.W. 1963. An algorithm for least-squares estimation of nonlinear parameters. J. Soc. Ind. Appl. Math. 11:431–441.
Martin, M.J., B.E. Logan, W.P. Johnson, D.G. Jewett, and R.G. Arnold. 1996. Scaling bacterial filtration rates in different sized porous media. J. Environ. Eng. 122(5):407–415.
Mawdsley, J.L., A.E. Brooks, and R.J. Merry. 1996a. Movement of the protozoan pathogen *Cryptosporidium parvum* through three contrasting soil types. Biol. Fertil. Soils 21:30–36.
Mawdsley, J.L., A.E. Brooks, R.J. Merry, and B.F. Pain. 1996b. Use of a novel soil tilting table apparatus to demonstrate the horizontal and vertical movement of the protozoan pathogen *Cryptosporidium parvum* in soil. Biol. Fertil. Soils 23:215–220.
Medema, G.J., F.M. Schets, P.F.M. Teunis, and A.H. Havelaar. 1998. Sedimentation of free and attached *Cryptosporidium* oocysts and *Giardia* cysts in water. Appl. Environ. Microbiol. 64:4460–4466.
Meinders, J.M., H.C. van der Mei, and H.J. Busscher. 1995. Deposition efficiency and reversibility of bacterial adhesion under flow. J. Colloid Interface Sci. 176:329–341.
Olson, M.E., J. Goh, M. Phillips, N. Guselle, and T.A. McAllister. 1999. *Giardia* cyst and *Cryptosporidium* oocyst survival in water, soil, and cattle feces. J. Environ. Qual. 28:1991–1996.
Peeters, J.E., E. Ares Mazás, W.J. Masschelein, I. Villacorta-Martinez de Maturana, and E. Debacker. 1989. Effect of drinking water with ozone or chlorine dioxide on survival of *Cryptosporidium parvum* oocysts. Appl. Environ. Microbiol. 55:1519–1522.
Pieper, A.P., J.N. Ryan, R.W. Harvey, G.L. Amy, T.H. Illangasekare, and D.W. Metge. 1997. Transport and recovery of bacteriophage PRD1 in a sand and gravel aquifer: Effect of sewage-derived organic matter. Environ. Sci. Technol. 31(4):1163–1170.
Redman, J.A., S.B. Grant, T.M. Olson, and M.K. Estes. 2001. Pathogen filtration, heterogeneity, and the potable reuse of wastewater. Environ. Sci. Technol. 35:1798–1805.
Rose, J.B. 1988. Occurrence and significance of *Cryptosporidium* in water. J. Am. Water Works Assoc. 80:53–58.
Rose, J.B., C.P. Gerba, and W. Jakubowski. 1991. Survey of potable water supplies for *Cryptosporidium* and *Giardia*. Environ. Sci. Technol. 25:1393–1400.
Ryan, J.N., and M. Elimelech. 1996. Colloid mobilization and transport in groundwater. Colloids Surf. A 107:1–56.
Schijven, J.F., W. Hoogenboezem, S.M. Hassanizadeh, and J.H. Peters. 1999. Modeling of bacteriophages MS2 and PRD1 by dune discharge at Castricum, Netherlands. Water Resour. Res. 35(4): 1101–1111.
Simoni, S.F., H. Harms, T.N.P. Bosma, and A.J.B. Zehnder. 1998. Population heterogeneity affects transport of bacteria through sand columns at low flow rates. Environ. Sci. Technol. 32(14):2100–2105.
Simunek, J., K. Huang, M. Sejna, and M.Th. van Genuchten. 1998. The HYDRUS-1D software package for simulating the one-dimensional movement of water, heat, and multiple solutes in variably-saturated media. Version 2.0. IGWMC-TPS-70. Int. Ground Water Modeling Center, Colorado School of Mines, Golden.
Sobsey, M.D. 1989. Inactivation of health-related microorganisms in water by disinfection processes. Water Sci. Technol. 21:179–195.
Tufenkji, N., J.A. Redman, and M. Elimelech. 2003. Interpreting deposition patterns of microbial particles in laboratory-scale column experiments. Environ. Sci. Technol. 37:616–623.
Walker, M.J., and C.D. Montemagno. 1999. Sorption of *Cryptosporidium parvum* oocysts in aqueous solution to metal oxide and hydrophobic substrates. Environ. Sci. Technol. 33:3134–3139.
Van Genuchten, M.Th. 1980. A closed-form equation for predicting the hydraulic conductivity of unsaturated soils. Soil Sci. Soc. Am. J. 44:892–898.